J. Fluid Mech. (1978), *vol.* 87, *part* 3, *pp.* 583–606
Printed in Great Britain

The interaction between vortex-array representations of free-stream turbulence and semi-infinite flat plates

By H. ROGLER

Department of Mechanical and Aerospace Engineering,
Case Western Reserve University, Cleveland, Ohio†

(Received 9 December 1976 and in revised form 29 August 1977)

Free-stream turbulence is modelled by a low-intensity array of vortices where the vorticity is distributed continuously throughout the flow. This vorticity approaches and convects along a semi-infinite flat plate and the structure of the free-stream disturbances is altered by the impermeability condition at the plate. The analysis consists of tracking the vorticity as it convects with the uniform mean flow, determining the stream function induced by that vorticity field without imposing the impermeability condition, and finally superimposing an irrotational flow field which effects impermeability. The bisecting of a vortex as it encounters the plate yields a pair of vortices which rotate in the same direction. The combined heights of these vortices are less than the height of the original vortex. Small segments of a vortex which has been cut by the plate, but not through its centre, are completely absorbed by neighbouring vortices. Far from the leading edge in any direction, the disturbance pressure is $O(\rho q^2)$, where q is the characteristic disturbance speed, and the streamline patterns convect with the mean flow. Near the leading edge, the fluctuating pressure is $O(\rho q U_\infty)$ because of unsteady vortex distortion and the velocity correlations reveal that Taylor's hypothesis is not valid. These correlations are based on averages over time and over all possible orientations of the vortex array. Vortex structures based on iso-vorticity contours are sometimes quite different from the structures based on disturbance streamlines.

1. Introduction

Fluids in motion often contain turbulence or other unsteady rotational structures which propagate by convection and other mechanisms, and there are many interactions between the patches or filaments of vorticity in the free-stream flow. If a plate, airfoil or other impermeable body is immersed in that fluctuating vortical flow, then new features arise as the eddies or vortices 'collide' with the plate and adjust to the impermeability and no-slip conditions at the surface and the shearing environment of the boundary layer developing along the plate. The features examined in this study are the effects of the impermeability condition on the unsteady flow field and pressure field.

An inviscid study of a semi-infinite plate in a flow field with rotational free-stream disturbances yields many results useful for later studies of the effects of free-stream unsteadiness and rotationality on boundary layers, on heat transfer and skin friction along the plate, and on laminar–turbulent boundary-layer transition. The unsteady

† Present address: Department of Aerospace Engineering, University of Southern California, Los Angeles.

pressure distribution along the plate, while serving as necessary input into boundary-layer analyses, also would be of importance for the aerodynamic loading and moments on the plate, just as for a plate of finite length modelling a thin airfoil. If the plate is 'very long' relative to the wavelength of the free-stream disturbance, however, then the aerodynamic loading on a semi-infinite plate would be similar in some respects to the loading on a plate of finite length but without the complications of the unsteady bound circulation and the oscillating vortex sheets downstream of a plate of finite length, which are associated with the trailing edge. Finally, the unsteady pressure field established when the free-stream disturbances impinge on a plate would be required as the forcing function which links the incompressible pressure field with the sound generated.

Probably the most common rotational free-stream disturbance is turbulence, but other forms are the vorticity shed from upstream bodies in the form of wakes, vortex streets, vortex sheets and rings, or other patches or layers of vorticity convected along in the flow. Mainly guided by the many observations that eddies or other vortical structures exist in turbulence and with the intent of modelling some of their unsteady rotational features, we represent the turbulence by an array of vortices. Rather than resorting to empirical modelling of the Reynolds stresses, eddy viscosities or mixing lengths in the mean equations, rather than considering the dynamical equations for the disturbance correlations, and rather than considering one Fourier mode or *plane wave* interacting with the body, we seek the unsteady interaction of this *vortex array* with a semi-infinite plate. While the objective is to determine the instantaneous flow field, certain averaged properties such as the velocity correlations are obtained from suitable averages of the unsteady flow field.

In the remainder of this section, some properties of vortex arrays are presented and previous studies with vortex arrays are summarized. The two-wavenumber model

$$u'(x,y,t) = -q_1 \cos(\beta y + y_1) \sin[\alpha(x-ct)+x_1] = -\psi'_y, \tag{1.1}$$

$$v'(x,y,t) = q_2 \sin(\beta y + y_1) \cos[\alpha(x-ct)+x_1] = \psi'_x, \tag{1.2}$$

$$\psi'(x,y,t) = (q_1/\beta) \sin(\beta y + y_1) \sin[\alpha(x-ct)+x_1], \tag{1.3}$$

$$\zeta'(x,y,t) = v'_x - u'_y = -(\alpha^2+\beta^2)\psi' = \nabla^2\psi' \tag{1.4}$$

for the velocities, stream function and vorticity represents an array of non-decaying vortices with rectangular boundaries which propagates at speed c in the x direction. x_1 and y_1 are phase angles or shifting parameters in the x and y directions. Continuity is satisfied if the amplitudes and wavenumbers are related by

$$-q_1\alpha + q_2\beta = 0. \tag{1.5}$$

Direct substitution of the stream function $\psi = -U_\infty y + \psi'$ into the inviscid equation

$$\left\{\frac{\partial}{\partial t} - \frac{\partial\psi}{\partial y}\frac{\partial}{\partial x} + \frac{\partial\psi}{\partial x}\frac{\partial}{\partial y}\right\}\nabla^2\psi = 0 \tag{1.6}$$

gives $c \equiv U_\infty$, i.e. the vortices convect with the *mean* flow. Additionally, since the velocity field also convects with the mean flow, two distinct balances arise in the Euler

equations: (1) the balance between the linear inertial terms and (2) the balance between the nonlinear and pressure-gradient terms, i.e.

$$\underbrace{\frac{\partial u_i'}{\partial t}+U_\infty\frac{\partial u_i'}{\partial x_1}}_{\text{balance 1}}+\underbrace{u_j'\frac{\partial u_i'}{\partial x_j}}_{\text{balance 2}}=-\frac{1}{\rho}\frac{\partial p'}{\partial x_i}\quad\text{for}\quad i,j=1,2. \tag{1.7}$$

These balances are exact in the limit of infinite Reynolds number and approximately correct when the Reynolds number based on the length or width of the vortex (whichever is smaller) is sufficiently large that spatial decay† is negligible. Except that the intensity $(q_1^2+q_2^2)^{\frac{1}{2}}/U_\infty$ cannot be so large that compressibility effects are significant, the form of the array and the satisfaction of Taylor's hypothesis are not limited to low intensities.

In the present work, the vortices are square and convect with the mean flow. The amplitudes and wavenumbers in the two directions are equal. The two-dimensionality and square geometry of the vortices have been adopted for simplicity. Three-dimensional skewed models of this array were considered by Rogler & Reshotko (1974, hereafter referred to as V). Both a cubical non-convected model and a two-dimensional model with different amplitudes in different directions were considered by Taylor (1936) to obtain the mean-square pressure fluctuation in an eddying flow. Taylor & Green (1937) also used arrays of cubical vortices to illustrate the evolution of smaller vortices from larger ones, and several other studies summarized by Van Dyke (1977) have extended these results.

If the characteristic length Λ (the vortex 'diameter' or half-wavelength), the characteristic disturbance speed q (the maximum speed at the four midpoints of the vortex boundary‡), the characteristic time Λ/U_∞ (the time required for a vortex to convect a distance of one diameter), the characteristic stream function $q\Lambda$ and the characteristic vorticity q/Λ are introduced, then the dimensionless disturbance fields are

$$u^{(a)}=-\cos(\pi y+y_1)\sin\pi(x-t)=-\psi_y^{(a)}\quad\text{(longitudinal velocity)}, \tag{1.8}$$

$$v^{(a)}=\sin(\pi y+y_1)\cos\pi(x-t)=\psi_x^{(a)}\quad\text{(lateral velocity)}, \tag{1.9}$$

$$\psi^{(a)}=\pi^{-1}\sin(\pi y+y_1)\sin\pi(x-t)=-\zeta^{(a)}/2\pi^2\quad\text{(stream function)}, \tag{1.10}$$

$$\zeta^{(a)}=-2\pi\sin(\pi y+y_1)\sin\pi(x-t)=-2\pi^2\psi^{(a)}\quad\text{(vorticity)}, \tag{1.11}$$

as illustrated in figure 1. The superscript (a) emphasizes that these are the disturbance variables which exist in the *absence* of any plate or other body immersed in the flow. Note that all wavenumbers and the frequency are equal. The parameter y_1 shifts the array in the y direction. When $y_1=0$, the x axis coincides with the boundary between two rows of vortices; if $y_1=\frac{1}{2}\pi$, then the x axis bisects one row of vortices through their centres, as shown in figure 2. Other values are also possible, although attention can be restricted to the range $0\leqslant y_1\leqslant 2\pi$ because of the periodic character. The phase angle x_1 in (1.1)–(1.4) is neglected since the time variable is available to control the x positioning of the array.

† For *temporal* decay of a homogeneous array, the viscous terms combine with the linear inertial terms to yield again two distinct balances, but now valid for all Reynolds numbers.

‡ The maximum disturbance speed is twice the r.m.s. value when averaging is carried out over the cross-sectional area of one vortex.

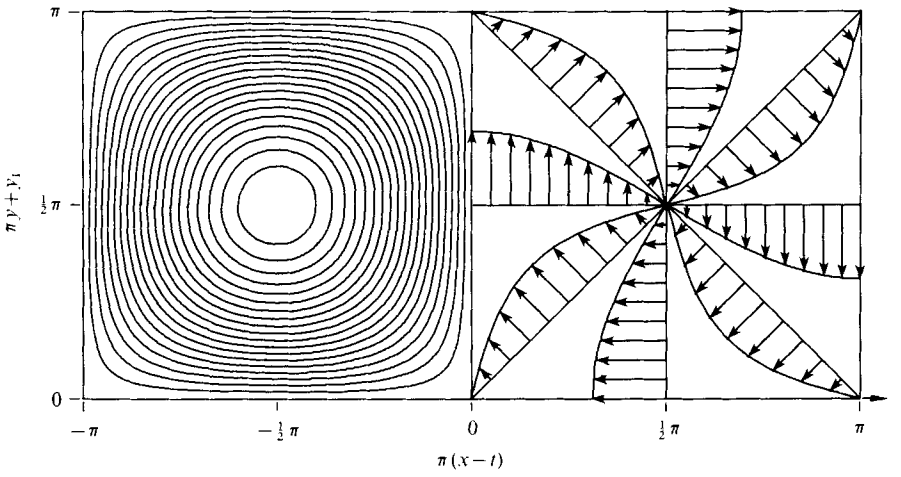

FIGURE 1. Disturbance streamlines for a harmonic vortex and disturbance velocity profiles for its counter-rotating neighbour. The streamlines are also contours of constant vorticity and disturbance pathlines.

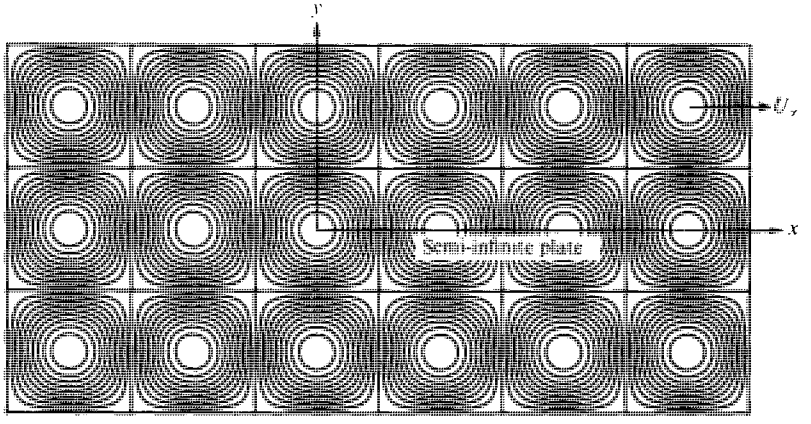

FIGURE 2. Contours of constant vorticity for an array of high Reynolds number, low-intensity vortices convecting beside a semi-infinite plate. The shifting parameter governing the y orientation of the array with respect to the plate has the value $y_1 = \frac{1}{2}\pi$ while the time $t = \frac{1}{2}$.

Near the centres of these vortices, the fluid is in nearly solid-body (wheel-like) rotation and the vorticity diminishes to zero along the square boundaries. Stagnation points occur at the centre and four corners of each vortex. If averaging is carried out over one time period and over the range $0 \leqslant y_1 \leqslant 2\pi$ of the shifting parameter, then this array is homogeneous and isotropic (in a two-dimensional sense) and has a zero Reynolds stress.

Other properties of this array are presented in V and Rogler & Reshotko (1975, hereafter VI), where the interaction of an array with a parallel-flow Blasius layer in a linearized study included the effects of a non-uniform mean shear, impermeability and the no-slip condition. Rogler (1975*a*, hereafter II) includes the case of an array of vortices propagating past plates of finite length. An initial-value problem for a vortex array impulsively cut by a plate is presented in Rogler (1975*b*, hereafter III). In

Rogler (1977, hereafter IV), the stream function is specified along the y axis and thus no upstream influence of the leading edge on the unsteady flow is permitted. This restriction is eliminated in the present work, where the stream function is specified far upstream.

In the next section, we outline the conditions under which the disturbance vorticity convects with the mean flow. In §3, an explicit solution for the stream function is obtained for unsteady flow past a semi-infinite plate. In §4, 'double-averaging' is introduced and applied to the two-point velocity correlations. In §5, the flow field is found for the region far downstream of the leading edge. Several complications and observations associated with interpreting eddying flow fields are illustrated in §6. In §7, the disturbance pressure is obtained via the unsteady linearized Bernoulli equation. Results are summarized in §8.

2. Mean and disturbance vorticity

Vorticity in a two-dimensional flow with constant viscosity and density is governed by the equation

$$\frac{\partial \zeta}{\partial t} + U\frac{\partial \zeta}{\partial x} + V\frac{\partial \zeta}{\partial y} = \nu\left(\frac{\partial^2 \zeta}{\partial x^2} + \frac{\partial^2 \zeta}{\partial y^2}\right) \tag{2.1}$$

for the component of vorticity ζ in the z direction. When the vorticity and velocities are separated into mean and disturbance contributions, introduced into (2.1) and suitably averaged (over one time period if the disturbances are periodic), an equation governing the mean vorticity results. We now non-dimensionalize the mean equation using our experience with elementary boundary layers and the behaviour of vorticity disturbances away from boundaries to select characteristic variables. While the non-dimensionalizations are not uniformly valid throughout the many contrasting regions and layers, a useful framework follows from the substitutions

$$\left.\begin{aligned} x = Lx_2, \quad y = \delta^* y_2, \quad \bar{\zeta} = U_\infty \bar{\zeta}/\delta^*, \quad \bar{U} = \bar{U}_\infty \bar{U}, \quad \bar{V} = \delta^* U_\infty \bar{V}/L \\ \text{for mean quantities and their derivatives,} \\ x = \Lambda x, \quad y = \Lambda y, \quad \zeta' = q\zeta'/\Lambda, \quad u' = qu', \quad v = qv', \quad t = \Lambda t/U_\infty \\ \text{for disturbance quantities and their derivatives.} \end{aligned}\right\} \tag{2.2}$$

To remind us that the averaging of products depends on the phase relationships between the disturbance quantities being averaged, we further introduce a constant c of magnitude $0 \leqslant c \leqslant 1$, where c may be much less than one since correlations of nearly 'out-of-phase' variables may be much less than the products of the reference quantities. δ^* is the boundary-layer displacement thickness, q is the characteristic disturbance speed and Λ is the characteristic scale of the vorticity disturbance. Under this non-dimensionalization, the mean vorticity equation is

$$\bar{U}\frac{\partial \bar{\zeta}}{\partial x_2} + \bar{V}\frac{\partial \bar{\zeta}}{\partial y_2} + c\frac{\delta^*}{\Lambda}\frac{q^2}{U_\infty^2}\underbrace{\left(\overline{u'\frac{\partial \zeta'}{\partial x}}\right)}_{(a)} + \underbrace{\left(\overline{v'\frac{\partial \zeta'}{\partial y}}\right)}_{(b)} = \underbrace{\frac{1}{R_{\delta^*}^2}\frac{\partial^2 \bar{\zeta}}{\partial x_2^2}}_{(c)} + \frac{\partial^2 \bar{\zeta}}{\partial y_2^2}, \tag{2.3}$$

where $\partial\bar{\zeta}/\partial t = 0$. For $c\delta^* q^2/\Lambda U_\infty^2 \ll 1$ and $R_{\delta^*}^2 \ll 1$, we neglect terms (a), (b) and (c) relative to the other terms, which are of unit order. Under these conditions, mean vorticity exists near a body submerged in a field of vorticity disturbances as a result of

the convection and diffusion of vorticity originating at the boundary in the usual form of a boundary layer. Outside the boundary layer, the mean flow remains irrotational if it is assumed that a uniform mean flow exists far upstream.

The disturbance vorticity equation is now

$$\underset{(d)}{\frac{\partial\zeta'}{\partial t}}+\underset{(d)}{\overline{U}\frac{\partial\zeta'}{\partial x}}+\frac{1}{R_{\delta^*}}\underset{(e)}{\overline{V}\frac{\partial\zeta'}{\partial y}}+\frac{\Lambda^2}{\delta^{*2}}\left(\frac{1}{R_{\delta^*}}\underset{(f)}{u'\frac{\partial\bar{\zeta}}{\partial x_2}}+\underset{(g)}{v'\frac{\partial\bar{\zeta}}{\partial y_2}}\right)$$

$$+\frac{q}{U_\infty}\left[\underset{(h)}{u'\frac{\partial\zeta'}{\partial x}}+\underset{(i)}{v'\frac{\partial\zeta'}{\partial y}}-c\left(\underset{(j)}{\overline{u'\frac{\partial\zeta'}{\partial x}}}+\underset{(k)}{\overline{v'\frac{\partial\zeta'}{\partial y}}}\right)\right]=\frac{1}{R_\Lambda}\left(\underset{(l)}{\frac{\partial^2\zeta'}{\partial x^2}}+\underset{(m)}{\frac{\partial^2\zeta'}{\partial y^2}}\right), \quad (2.4)$$

where $R_\Lambda = U_\infty \Lambda/\nu$. We begin our simplification by restricting attention to regions outside the mean boundary layer where $\overline{U} = 1$ in term (d) and neglect the $O(1/R_{\delta^*})$ term (e), which may be of importance near the leading edge. Outside the boundary layer, terms (f) and (g) are identically zero in the irrotational mean flow.

Neglecting the nonlinear terms

For low-intensity disturbances, i.e. $q/U_\infty \ll 1$, we eliminate the nonlinear terms (h) and (i) and their averages (j) and (k). We have shown previously that these terms vanish identically in the free stream. In the region near the wall, although not all the nonlinear terms vanish, we can estimate *a posteriori* their accumulative influence downstream of the leading edge. From III, the nonlinear terms are

$$\frac{q}{U_\infty}\left(u'\frac{\partial\zeta'}{\partial x}+v'\frac{\partial\zeta'}{\partial y}\right)=\frac{q}{U_\infty}\pi^2\sin y_1\, e^{-\pi y}\sin 2\pi(x-t)\left[\sin(\pi y+y_1)+\cos(\pi y+y_1)\right]. \quad (2.5)$$

Note that the nonlinear terms vanish far away from the wall and also when $y_1 = 0$. When averaged over one time cycle $0 \leqslant t \leqslant 2$, terms (j) and (k) vanish in (2.4). When $y_1 = \frac{1}{2}\pi$, $\pi(x-t) = \frac{1}{4}\pi$ and $y = 0$, the above terms reduce to $\pi^2 q/U_\infty$.

To estimate the accumulative effects of these terms, we ask, 'At what distance L downstream have these terms "significantly altered" the vorticity field (say by some fraction ϵ of the vorticity maximum)?' Away from the leading edge, the above influence is constant and will be integrated over the interval $0 < x < L$. The result is

$$L = \epsilon U_\infty/q. \quad (2.6)$$

Hence the distance downstream where a 'significant' rearrangement of vorticity has occurred is inversely proportional to the intensity. If $\epsilon = 0{\cdot}1$ (i.e. the vorticity field has been changed by 10 % of $\zeta_{\max}$) and the intensity is $q/U_\infty = 0{\cdot}01$, then $L = 10$ vortex diameters. This estimate is conservative since y_1 can take on all values in the range $0 \leqslant y_1 < 2\pi$.

In a small region very near the leading edge, the disturbances velocities are large and nonlinear rearrangement of vorticity will be significant. However, this region can be made small by reducing the intensity of the disturbances. As long as one stays outside this region 'very near' the leading edge and outside the 'very thin' layer along the plate downstream of this region, these inviscid nonlinear effects should not be significant. Rogler (1974, hereafter I) is a study of a single potential vortex in a uniform mean flow whose trajectory is affected by these nonlinearities, which are shown

to be negligible if the parameter $|\Gamma/2\pi bU_\infty|$ is small, where Γ is the circulation of the vortex and b is its lateral distance from the plate when any effects on the trajectory are neglected.

Neglecting the viscous terms

For large Reynolds numbers based on the vortex diameter, i.e. $R_\Lambda \equiv 1/\epsilon \gg 1$, we neglect the viscous terms (l) and (m). Away from any wall, Rogler & Reshotko (1976, hereafter VII) demonstrated that the vorticity amplitude decays as $\exp(-f_1 \pi x)$, where

$$f_1(\epsilon) = 2\pi\epsilon - 12\pi^3\epsilon^3 + O(\epsilon^5) \quad \text{as} \quad \epsilon \to 0. \tag{2.7}$$

The first term in the series represents the temporally decaying solution by Taylor (1923) transformed to a spatially decaying array by using Taylor's hypothesis. Expanding the exponential shows that the amplitude is diminished by a fraction f in the dimensionless distance

$$L/\Lambda = fR_\Lambda/2\pi^2. \tag{2.8}$$

For a vortex of diameter 1m in air at 30 °C convecting at 100 m/s with $f = 0{\cdot}1$,

$$R_\Lambda = 6 \times 10^6 \quad \text{and} \quad L/\Lambda = 3 \times 10^4,$$

i.e. the vorticity amplitude decays by 10 % in a distance of 30000 ms. For a 1 cm vortex in water, $R_\Lambda = 1{\cdot}25 \times 10^6$ and $L = 62$ m.

This decay rate differs appreciably from the decay of turbulence since it represents the decay of a single-wavenumber disturbance. In turbulence, viscous decay occurs in the high wavenumber dissipation subrange, with transfer from the lower wavenumbers arising via nonlinear interactions. Hunt (1973) developed a statistical theory for the linearized inviscid distortion of three-dimensional turbulence about two-dimensional bluff bodies, including the effects of vortex stretching, then applied his formulation to the case of flow past a circular cylinder, neglecting any mean boundary layers. He estimated the decay length based on the Kolmogorov dissipation length. The spirit of his estimate is believed proper for turbulence, although the effects of the nearby wall on the dissipation length should be taken into account.

For regions near the plate, but not within the sublayer, III showed that the rearranged flow field near the plate decays about twice as fast as in the free stream, so an additional factor of 2 in the denominator of (2.8) is warranted. A much greater viscous effect arises in the viscous sublayer near the boundary. For disturbances of length λ (perhaps smaller than Λ) propagating at speed c (generally less than U_∞), if

$$\lambda/c = O(\Lambda/U_\infty)$$

then a balance between the unsteady and y viscous terms yields the estimate that the thickness of the sublayer is

$$\delta_s^*/\Lambda = O(R_\Lambda^{-\frac{1}{2}}), \tag{2.9}$$

which would be very small for the large Reynolds number cases of interest herein.

This estimate is based on the assumption that the mean flow is at rest near the wall, reflecting the smallness of the mean velocity in the boundary layer near the wall. The result is a viscous sublayer which diffuses outwards in the characteristic time Λ/U_∞. However, if the mean flow is uniform everywhere, as would arise if the surface were allowed to move with the mean flow and consequently no mean boundary layer

developed, then the character of the viscous layer is different. The relevant time scale is now L/U_∞, which is the time required for a vortex to convect from the leading edge (where the viscous layer begins diffusing) downstream to the position L of interest.

For an observer moving with the free stream, balancing the unsteady and y viscous terms yields an estimate of the viscous-layer thickness of

$$\delta_v^*/L = O(R_L^{-\frac{1}{2}}) \quad \text{or} \quad \delta_v^*/\Lambda = O((L/\Lambda R_\Lambda)^{\frac{1}{2}}). \tag{2.10}$$

Consequently, the thickness of this *unsteady* viscous layer grows parabolically in the downstream direction as does an ordinary boundary layer if the mean flow is everywhere uniform.

With either estimate, depending on which mean flow exists, we shall restrict attention to regions outside both the mean and the unsteady viscous layer.

The possibility remains that the vorticity field *inside* the boundary layer, which we acknowledge to have been altered by the terms (*d*), (*g*) and perhaps others, will alter the vorticity field *outside* the boundary layer. V and VI reveal that this influence exists, but if the displacement thickness is small with respect to the vortex diameter, i.e. $\pi\delta^*/\Lambda \ll 1$, then the effect is small. Although that work was based on disturbances which propagate with the free stream and other phase speeds are also possible, we shall apply that conclusion here and thus neglect any influence the boundary layer may have on the *vorticity* field just outside the boundary layer.

Little can be said at this time regarding unsteady viscous effects at a *sharp* leading edge. The steady case was considered analytically by Carrier & Lin (1948) and numerically by Van de Vooren & Dijkstra (1970). Others have studied oscillating flows about blunt cylindrical bodies under high Reynolds number conditions with thin unsteady stagnation boundary layers and with irrotational disturbances of form $\epsilon \exp(i\omega t)$, but their relationships to flows about thin blunt plates with rotational travelling fluctuations are unclear.

The unseparated solution which we seek with a plate of zero thickness is believed to be valid for a thin plate with a streamlined nose and with low-intensity fluctuations. The thickness of the plate should be small relative to the vortex scale so that negligible distortion of the vorticity field occurs, but sufficiently thick so that the flow about the leading edge remains small. The intensity of the free-stream fluctuations as well as the nose shape and other factors will dictate the magnitude of the flow about the leading edge, which can be made as small as desired as long as the plate thickness does not vanish. How small q/U_∞ and how large the thickness must be to eliminate separation must await further research.

Simplified vorticity equation

In summary, under the conditions $q/U_\infty \ll 1$, $R_\Lambda \gg 1$ and $k = \pi\delta^*/\Lambda \ll 1$, the mean flow can everywhere be modelled by its irrotational free-stream value with the understanding that the solution is not valid in the viscous sublayer. Should the condition $k \ll 1$ not be satisfied, then the solution would not be valid either in or near the boundary layer. The disturbance vorticity equation now reduces to

$$\partial\zeta'/\partial t + \partial\zeta'/\partial x = 0, \tag{2.11}$$

with solution

$$\zeta'(x, y, t) = \zeta'(x - t, y) = \zeta^{(a)}, \tag{2.12}$$

i.e. the *vorticity* field is unaffected by the presence of the plate and convects with the uniform mean flow. The contours of constant vorticity for flow past a semi-infinite plate are shown in figure 2. However, through the impermeability condition, the velocity field and stream function will be altered by the plate.

This result is analogous to the 'rapid-distortion' theories of Prandtl (1933), Taylor (1935) and Batchelor & Proudman (1954), who addressed the distortion of turbulence arising from quasi-one-dimensional changes in the mean flow field such as a contraction in a wind tunnel. Hunt (1973) also developed an analogous result for the vorticity convected by the irrotational mean flow past a cylinder.

Although the source of the vorticity disturbances is unimportant, conceptually it may be helpful to assume that a 'screen' located upstream of the plate generates these vortices. In this inviscid analysis, the geometrical factor specifying the position of the screen is eliminated by moving it an unlimited distance upstream. Hence these vortices are input at 'minus infinity' and convect downstream. They reach the plate after an unlimited time, the initial transient effects vanish and a steady-state oscillation is established which is the objective of the ensuing analysis.

3. Disturbance stream function

While the disturbance vorticity convects with the mean flow and is unaffected by the presence of the plate, the stream function and velocities in some region near the plate will be affected by the impermeable boundary. Since no vorticity is generated when the vortices 'collide' with the plate, the disturbance stream function ψ' with the plate present is related to that vorticity by Poisson's equation

$$\nabla^2\psi' = \zeta^{(a)}. \tag{3.1}$$

This stream function is now separated into two components

$$\psi' = \psi^{(a)} - \psi^{(i)}, \tag{3.2}$$

where $\psi^{(a)}$ is the stream function for the free-stream disturbances in the absence of the plate as given by (1.10) and $\psi^{(i)}$ is the *irrotational, impermeability* stream function, which represents the irrotational alteration to those free-stream disturbances arising because of the impermeability condition. Hence this stream function satisfies Laplace's equation

$$\nabla^2\psi^{(i)} = 0 \tag{3.3}$$

and, when combined with $\psi^{(a)}$ in (3.2), satisfies impermeability.

Now, at the plate $\psi' = \psi_0$, which may be a function of the parameters of the problem and time, but is not dependent on the position along the plate. Hence, if

$$\psi' = \psi_0 = \psi^{(a)} - \psi^{(i)}$$

along the plate, then the appropriate condition on Laplace's equation at the plate is $\psi^{(i)} = \psi^{(a)} - \psi_0$. If $\psi^{(a)}$ is evaluated along $y = 0$, then the boundary condition along the plate becomes

$$\psi^{(i)} = \pi^{-1}\sin y_1 \sin\pi(x-t) - \psi_0(t) \quad \text{for} \quad 0 < x < \infty. \tag{3.4}$$

Since the impermeability condition is applied only along the plate, this condition is not applicable upstream of the plate, i.e. for negative x. Furthermore, for this elliptic

problem, the conditions that $\psi^{(i)}$ vanishes for large distances normal to the plate and far upstream must be added. These conditions reflect our intuition that the influence of the plate is limited to some region near the plate and vanishes far away. Finally, far downstream of the leading edge but near the plate, the solution must be bounded.

For the present formulation, a direct solution of Laplace's equation subject to a Dirichlet condition only along the $+x$ axis would be difficult. Instead, we exploit the symmetry about the x axis, add the homogeneous Neumann condition along the $-x$ axis, i.e.

$$\partial\psi^{(i)}/\partial y = 0 \quad \text{for} \quad y = 0, \quad -\infty < x < 0, \tag{3.5}$$

and restrict attention to the half-plane $y \geqslant 0$ while solving for $\psi^{(i)}$.

To alleviate the problem of split boundary conditions along the x axis, we conformally map the half-plane $y \geqslant 0$ onto the quarter-plane $0 \leqslant \xi < \infty$, $0 \leqslant \eta < \infty$ through the transformation

$$\zeta \equiv \xi + i\eta = (x+iy)^{\frac{1}{2}} \equiv z^{\frac{1}{2}}. \tag{3.6}$$

If $z = re^{i\theta}$, where $0 \leq \theta < 2\pi$, then $z^{\frac{1}{2}} = r^{\frac{1}{2}} e^{\frac{1}{2}i\theta}$ is the intended root. Under this transformation, the $+x$ axis maps onto the $+\xi$ axis and the $-x$ axis maps onto the $+\eta$ axis. In this co-ordinate system, the boundary-value problem is

$$\psi^{(i)}_{\xi\xi} + \psi^{(i)}_{\eta\eta} = 0, \tag{3.7}$$

$$\psi^{(i)} = \pi^{-1} \sin y_1 \sin \pi(\xi^2 - t) - \psi_0(t) \quad \text{for} \quad \eta = 0, \quad \xi > 0, \tag{3.8}$$

$$\psi^{(i)}_{\xi} = 0 \quad \text{for} \quad \eta > 0, \quad \xi = 0, \tag{3.9}$$

$$\psi^{(i)} \to 0 \quad \text{as} \quad \eta \to \infty, \tag{3.10}$$

$$\psi^{(i)} \text{ bounded near the plate as } \xi \to \infty. \tag{3.11}$$

The origin is a singular point of the transformation and is excluded.

The solution of this problem can be extracted by applying a cosine integral transform in the ξ direction,

$$\hat{\psi}^{(i)}(s, \eta) = \left(\frac{2}{\pi}\right)^{\frac{1}{2}} \int_0^\infty \psi^{(i)}(\xi, \eta) \cos s\xi \, d\xi, \tag{3.12}$$

to Laplace's equation and the boundary conditions, solving the resultant ordinary differential equation, applying the boundary conditions, inverting the solution via the inverse transform

$$\psi^{(i)}(\xi, \eta) = \left(\frac{2}{\pi}\right)^{\frac{1}{2}} \int_0^\infty \hat{\psi}^{(i)}(s, \eta) \cos \xi s \, ds \tag{3.13}$$

(see, for example, Erdélyi *et al.* 1954, p. 158, noting errata), reversing the conformal transformation $\zeta^2 = z$ and introducing the symmetry relations

$$\sin(\pi z^*) = \sin^*(\pi z), \quad \cos(\pi z^*) = \cos^*(\pi z), S_2(\pi z^*) = S_2^*(\pi z), \quad C_2(\pi z^*) = C_2^*(\pi z),$$

where the asterisks denote complex conjugates and where S_2 and C_2 are the Fresnel integrals

$$\begin{matrix} S_2 \\ C_2 \end{matrix}(z) \equiv \frac{1}{(2\pi)^{\frac{1}{2}}} \int_0^z t^{-\frac{1}{2}} \begin{matrix} \sin \\ \cos \end{matrix}(t) \, dt. \tag{3.14}$$

To satisfy the condition $\psi^{(i)} \to 0$ as $\eta \to \infty$, $\psi_0 = 0$ is the value on the dividing streamline. The result for the stream function $\psi' = \psi^{(a)} - \psi^{(i)}$ is

$$\begin{aligned}\psi'(x,y,t,y_1) = {} & \pi^{-1}\sin(\pi y + y_1)\sin\pi(x-t) \\ & - \pi^{-1}\sin y_1 [\cos\pi t\,\mathscr{R}\{-\cos\pi z\, S_2(-\pi z) - \sin\pi z\, C_2(-\pi z) \\ & + \cos\pi z\, C_2(-\pi z) - \sin\pi z\, S_2(-\pi z) + \sin\pi z\} \\ & - \sin\pi t\ \mathscr{R}\{-\cos\pi z\, S_2(-\pi z) - \sin\pi z\, C_2(-\pi z) \\ & - \cos\pi z\, C_2(-\pi z) + \sin\pi z\, S_2(-\pi z) + \cos\pi z\}], \end{aligned} \tag{3.15}$$

where $\mathscr{R}\{A\}$ denotes the real part of A. If the arguments of the Fresnel integrals are left as shown, then the numerical evaluation follows without modification of standard complex square-root subroutines. For small values of z, the Fresnel integrals are evaluated from the power series at the zero point (see, for example, Abramowitz & Stegun 1965, p. 301). Asymptotic series can be used for large $|z|$.

Note first from (3.15) that when the plate coincides with a boundary between vortex rows ($y_1 = 0$) $\psi^{(i)} = 0$. Hence $\psi' = \psi^{(a)}$ and the plate does not influence the flow field since no change in the vortex structure is necessary to satisfy the impermeability condition. Second, note that the solution can be rewritten in the form

$$\begin{aligned}\psi' = {} & \psi_1(x,y)\sin y_1 \sin\pi t + \psi_2(x,y)\sin y_1\cos\pi t \\ & + \psi_3(x,y)\cos y_1 \sin\pi t + \psi_4(x,y)\cos y_1\cos\pi t. \end{aligned} \tag{3.16}$$

The functions ψ_i follow directly from (3.15) and are not presented here. Hence the flow field for any values of the shifting parameter y_1 and time t consists of a superposition of the four basic cases $(y_1, t) = (\frac{1}{2}\pi, \frac{1}{2}), (\frac{1}{2}\pi, 0), (0, \frac{1}{2})$ and $(0,0)$. The last two cases need not be considered since they represent the original array at two different times.

The disturbance streamlines for the case of a head-on collision between the plate and the vortex array ($y_1 = \frac{1}{2}\pi$) are shown in figure 3 for $t = \frac{1}{2}$. Also shown are the 'absence' or free-stream solution $\psi^{(a)}$ upstream of the plate and the 'far-downstream' solution to be developed later. Note the upstream influence of the plate. Also note that bisection of a vortex yields two vortices of combined height *less* than that of the original vortex and that this transition in height occurs smoothly as fluid is absorbed by the vortices above and below the bisected row. The closeness of the streamlines near the leading edge indicates high disturbance speeds. The case of a head-on collision at another time is illustrated in figure 4.

Figure 5 shows the streamlines for a skewed collision ($y_1 = -\frac{1}{4}\pi$). For this special value of y_1, the dissected piece above the plate is completely absorbed by the vortex above as the array propagates downstream. Tracing a few streamlines around, again note the transfer of fluid between vortices incited by the leading edge.

As the stream function is known, the velocities can be found as

$$u^{(i)} = -\psi^{(i)}_y = -i\sin y_1 F(z,t),$$

$$v^{(i)} = \psi^{(i)}_x = \sin y_1 F(z,t),$$

where $$\begin{aligned} F = {} & \sin\pi(z-t)\,[S_2(-\pi z) - C_2(-\pi z)] \\ & - \cos\pi(z-t)\,[S_2(-\pi z) + C_2(-\pi z) - 1] - \frac{\sin\pi t + \cos\pi t}{(-2z)^{\frac{1}{2}}} \end{aligned}$$

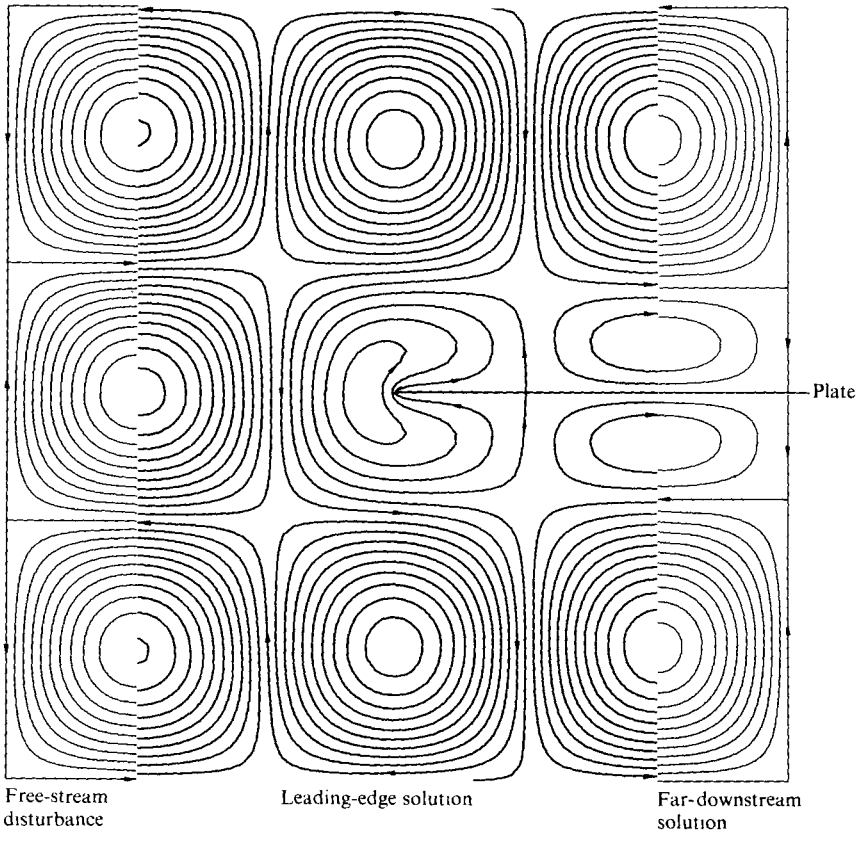

FIGURE 3. Disturbance streamlines for an array of vortices propagating along a semi-infinite plate for $t = \frac{1}{2}$ and $y_1 = \frac{1}{2}\pi$. The streamlines of the free-stream disturbance and the flow field far downstream of the leading edge are also shown for comparison.

As one approaches the leading edge along the $-x$ axis, since S_2 and C_2 are regular at the origin, the normal velocity behaves as

$$v^{(i)} = O(r^{-\frac{1}{2}}) \quad \text{as} \quad r \to 0 \quad \text{from the left,}$$

where r is the radial distance from the leading edge. This singularity in the irrotational flow at the leading edge has the same behaviour as the singularity at the trailing edge of a finite plate in unsteady aerodynamics (II) and as the leading-edge singularity in steady linearized airfoil theory. To satisfy our assumption of small amplitude disturbances, then, we must remain outside the 'very small' region of diameter $O(\epsilon^2)$ near the leading edge, where $\epsilon = q/U_\infty$.

To extract the asymptotic behaviour of $\psi^{(i)}$ far from the leading edge, separate expansions are required upstream and downstream of the leading edge. Upstream, the auxiliary functions (Abramowitz & Stegun 1965, p. 300)

$$f(z) = [\tfrac{1}{2} - S(z)]\cos(\tfrac{1}{2}\pi z^2) - [\tfrac{1}{2} - C(z)]\sin(\tfrac{1}{2}\pi z^2), \tag{3.17a}$$

$$g(z) = [\tfrac{1}{2} - C(z)]\cos(\tfrac{1}{2}\pi z^2) + [\tfrac{1}{2} - S(z)]\sin(\tfrac{1}{2}\pi z^2), \tag{3.17b}$$

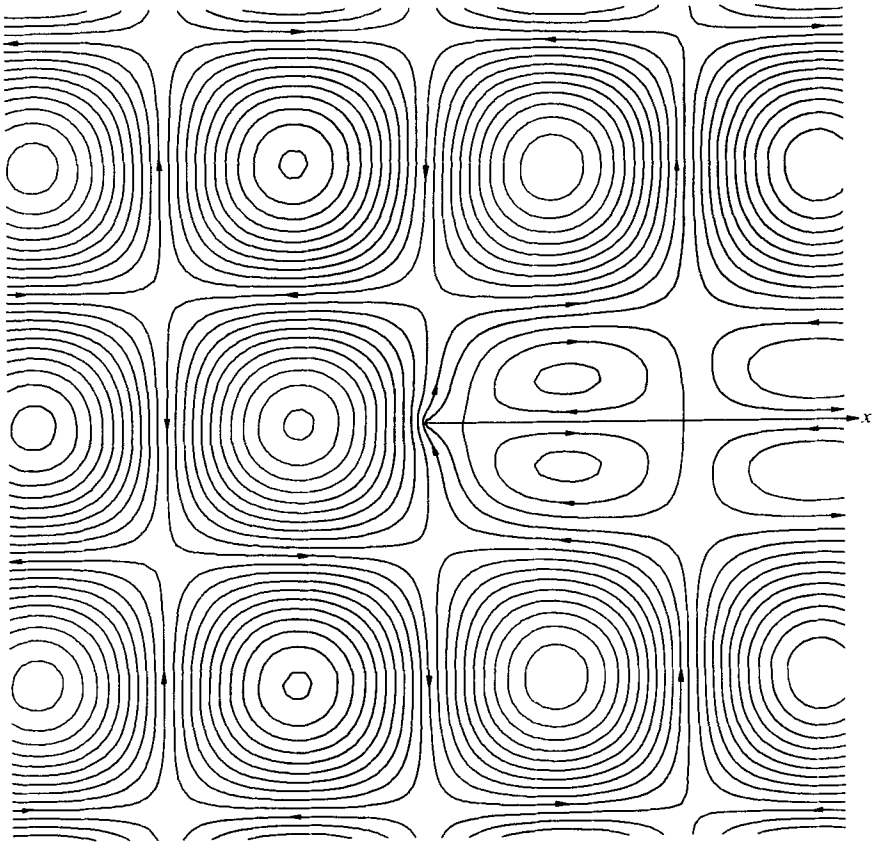

FIGURE 4. Disturbance streamlines for an array of vortices propagating along a semi-infinite plate for $t = 0$ and $y_1 = \frac{1}{2}\pi$.

where $C(z) = C_2(\frac{1}{2}\pi z^2)$ and $S(z) = S_2(\frac{1}{2}\pi z^2)$, are introduced into (3.15), yielding

$$\psi^{(i)} = \sin y_1 (\cos \pi t \mathscr{R}\{f-g\} - \sin \pi t \mathscr{R}\{f+g\})/\pi. \tag{3.18}$$

Upstream of the leading edge, the asymptotic expansions

$$\left.\begin{aligned} \pi z f(z) &\sim 1 + \sum_{m=1}^{\infty} (-1)^m . 1 . 3 \ldots (4m-1)/(\pi z^2)^{2m} \qquad (3.19a) \\ \pi z g(z) &\sim \sum_{m=0}^{\infty} (-1)^m . 1 . 3 \ldots (4m+1)/(\pi z^2)^{2m+1} \qquad (3.19b) \end{aligned}\right\} \quad \text{as} \quad z \to \infty, \quad |\arg z| < \tfrac{1}{2}\pi,$$

are applicable. Retaining only the first term gives

$$\psi^{(i)} \sim \frac{\sin y_1 \, |\sin \frac{1}{2}\theta| \, (\cos \pi t - \sin \pi t)}{2\pi^2 r^{\frac{1}{2}}} \quad \text{as} \quad r \to \infty, \tag{3.20}$$

where $z = re^{i\theta}$, $\pi < |\theta| < \frac{1}{2}\pi$ and hence $2^{-\frac{1}{2}} < |\sin \frac{1}{2}\theta| < 1$ in the upstream region. Note the slow algebraic, $O(r^{-\frac{1}{2}})$, decay of the plate influence. For times near $t = \frac{1}{4}$ and $\frac{5}{4}$, the coefficient $\cos \pi t - \sin \pi t$ is very small, and more rapidly decaying solutions are possible from higher-order terms.

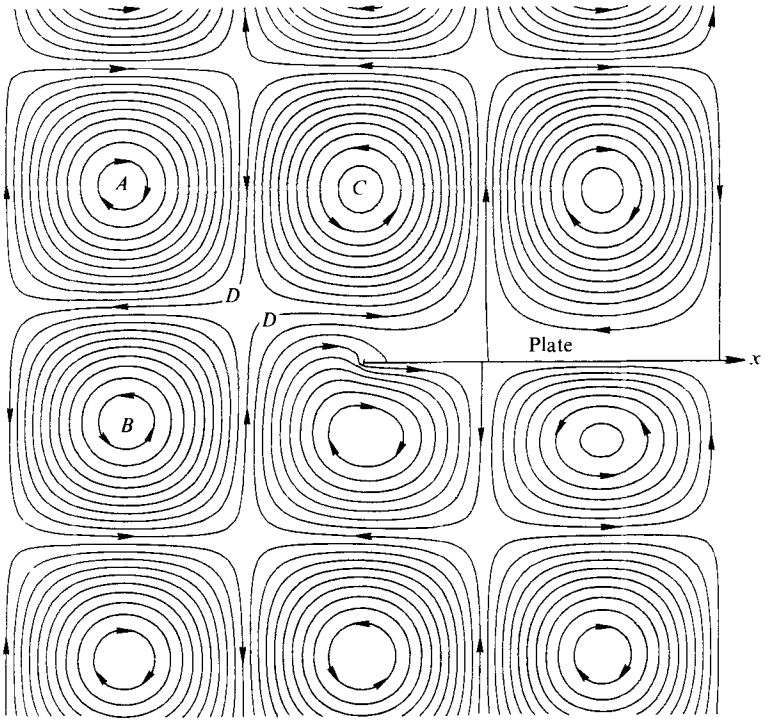

FIGURE 5. Disturbance streamlines for an array of vortices propagating along a semi-infinite plate for $t = \frac{1}{2}$ and $y_1 = -\frac{1}{4}\pi$.

Directly upstream of the plate, we form the ratio ϵ of the above contribution (for $t = \frac{3}{4}\pi$) to the maximum $1/\pi$ of the absence stream function at the centres of the vortices to provide an estimate of the distance upstream where the plate influence is negligible. The result is

$$r > \sin^2 y_1/\pi^2\epsilon^2. \tag{3.21}$$

If $\epsilon = 0{\cdot}1$ and $y_1 = \frac{1}{2}\pi$, then $r > 9$ diameters.

Either from the above asymptotic relation or, more directly, from (3.15) since the Fresnel integrals approach $\frac{1}{2}$ far upstream, $\psi^{(i)} \to 0$ as $r \to \infty$ and $\psi' \to \psi^{(a)}$ as expected since far upstream the free-stream disturbance should be recovered.

Far downstream, $C_2(-\pi z) \to -\frac{1}{2}i$ and $S_2(-\pi z) \to \frac{1}{2}i$ as $x \to \infty$ for positive values of y. After some manipulation, (3.15) reduces to

$$\psi' = \psi^{(a)} - \pi^{-1} \sin y_1 \, e^{-\pi y} \sin \pi(x-t). \tag{3.22}$$

Hence the solutions far upstream and far downstream differ. The latter solution will be derived in a more direct manner in § 5 and discussed there.

4. Double-averaged variables and correlations

We now 'double-average' the disturbance variables over one time period and over all possible values of the shifting parameter in the range $0 \leqslant y_1 \leqslant 2\pi$. For example, the double-average of u'^2 is

$$\overline{\overline{u'^2}}(x,y) = \frac{1}{2\pi}\int_{y_1=0}^{2\pi} \frac{1}{2}\int_{t=0}^{2} u'^2(x,y,t,y_1)\,dt\,dy_1. \tag{4.1}$$

Now $\overline{\overline{u'}} = \overline{\overline{v'}} = 0$, but generally $\overline{\overline{u'^2}} \neq 0$, $\overline{\overline{u'v'}} \neq 0$, etc. This averaging is equivalent to an ensemble average over an infinite number of realizations with time and the shifting parameter randomly specified. Although each realization is well ordered, the double-averaging partially alleviates the problem of the vortices lining up in straight rows and columns and more nearly models the time or ensemble averages of turbulence (V and VI). We proceed to extract as much information as possible from our analysis with one wavenumber.

The averaging is now used to form the two-point, one-time, longitudinal velocity correlation

$$f(r;x,y) \equiv \frac{\overline{\overline{u'(x,y,t,y_1)\,u'(x+r,y,t,y_1)}}}{[\overline{\overline{u'^2(x,y,t,y_1)}}]^{\frac{1}{2}}[\overline{\overline{u'^2(x+r,y_1,t)}}]^{\frac{1}{2}}}, \tag{4.2}$$

where r is the separation distance. The related two-time, one-point correlation transformed to a spatial correlation via Taylor's hypothesis $r = \Delta t$ (for a mean flow of unity) is

$$f_T(r;x,y) \equiv \frac{\overline{\overline{u'(x,y,t,y_1)\,u'(x,y,t-r,y_1)}}}{[\overline{\overline{u'^2(x,y,t,y_1)}}]^{\frac{1}{2}}[\overline{\overline{u'^2(x,y,t-r,y_1)}}]^{\frac{1}{2}}}, \tag{4.3}$$

where the subscript T denotes that Taylor's hypothesis has been introduced. Analogously, the double lateral correlations g and g_T associated with the normal disturbance velocity v' can be defined. We shall restrict attention to separations in the x direction since we are interested in comparing f with f_T and g with g_T to test the validity of Taylor's hypothesis.

If ψ' is known, u' and v' can be found and substituted into the correlations f_T and g_T, and the double-averaging carried out. The simple results are

$$f_T(r) = g_T(r) = \cos \pi r \tag{4.4}$$

for all reference points x and y.

Similarly, f and g can be found. The analysis is simplified if we write u' and v' as

$$u' = f_1 \sin y_1 \sin \pi t + f_2 \sin y_1 \cos \pi t + f_3 \cos y_1 \sin \pi t + f_4 \cos y_1 \cos \pi t, \tag{4.5}$$

$$v' = g_1 \sin y_1 \sin \pi t + g_2 \sin y_1 \cos \pi t + g_3 \cos y_1 \sin \pi t + g_4 \cos y_1 \cos \pi t, \tag{4.6}$$

where the functions $f_i(x,y)$ and $g_i(x,y)\,(i = 1, \ldots, 4)$ are given in the appendix. In terms of these functions, the double-mean quantities are

$$\overline{\overline{u'^2}}(x,y) = \tfrac{1}{4}[f_1^2(x,y) + f_2^2(x,y) + f_3^2(x,y) + f_4^2(x,y)], \tag{4.7}$$

$$\overline{\overline{u'^2}}(x+r,y) = \tfrac{1}{4}[f_1^2(x+r,y) + f_2^2(x+r,y) + f_3^2(x+r,y) + f_4^2(x+r,y)], \tag{4.8}$$

$$\begin{aligned}\overline{\overline{u'(x,y)\,u'(x+r,y)}} = \tfrac{1}{4}[&f_1(x,y)f_1(x+r,y) + f_2(x,y)f_2(x+r,y) \\ &+ f_3(x,y)f_3(x+r,y) + f_4(x,y)f_4(x+r,y)].\end{aligned} \tag{4.9}$$

If these expressions are substituted into equation (4.2) for the correlation $f(r;x,y)$, then that correlation can be numerically evaluated for any base point (x,y) and separation distance r of interest. Analogously, the functions g_i permit the evaluation of the two-point lateral correlation $g(r;x,y)$.

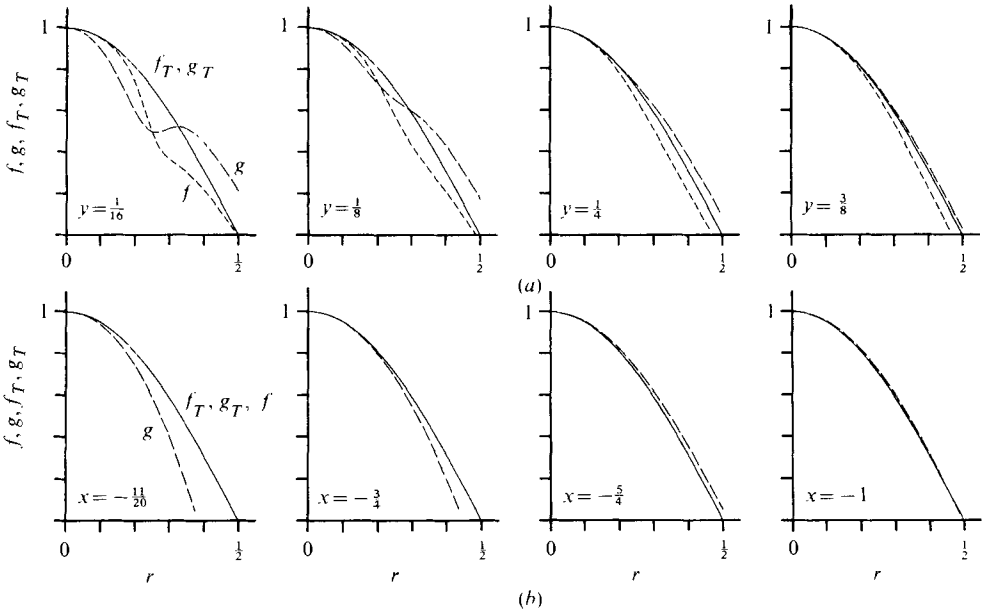

FIGURE 6. Two-point double-averaged longitudinal and lateral velocity correlations near the leading edge for (*a*) $x = -\frac{1}{4}$ and various y values and (*b*) $y = 0$ and various upstream x values.

The correlations f, f_T, g and g_T are plotted in figures 6 (*a*) and (*b*) for several reference points (x, y) upstream of and beside the leading edge. In figure 6 (*a*), the reference point is one-quarter of a vortex scale upstream of the leading edge and several distances normal to the plate. The disparities between f and f_T and between g and g_T reflect the distortion of the vortex structure effected by the plate. Whenever the disturbance streamlines are convected with the uniform flow without a change in structure, all four correlations vary as $\cos \pi r$. Whenever that pattern changes, Taylor's hypothesis is not valid and f_T and g_T differ from f and g, respectively.

As can be seen in figures 3–5, the distortion is large near the leading edge, and that result is reflected in figure 6 (*a*), particularly for $y = \frac{1}{16}$, by irregular correlations and a discrepancy between those correlations using Taylor's hypothesis and those using the exact velocities. As the distance from the leading edge increases, the four correlations become more similar. Since contributions from the pressure-gradient terms are invalidating Taylor's hypothesis near the leading edge, the contours of constant disturbance pressure shown in figure 10 and discussed later also indicate where the pattern convects and where it distorts.

In figure 6 (*b*), the correlations are shown for reference points directly upstream of the leading edge. As the reference point $(x, 0)$ approaches the leading edge, the lateral correlation diminishes. The longitudinal correlation for this special reference position $(y = 0)$ is unaffected by the plate because $\partial p'/\partial x = 0$ (to linear order) directly upstream of the plate, as shown in figure 10.

Generally, the assumptions under which Taylor's hypothesis is considered valid for a turbulent flow include a uniform mean flow, negligible viscous diffusion over the separation distance and low intensity, as noted by Taylor (1938), Corrsin & Uberoi (1952), Lin (1950, 1953), Hinze (1959, p. 40) and VII. While these assumptions are

identically satisfied in the present model, an additional restriction is that the flow cannot be in the 'immediate vicinity' of a leading edge, where impermeability causes distortion of the velocity field.

5. The solution far downstream

Far downstream of the leading edge, we expect its influence to vanish and the flow field to approach some unchanging pattern which convects with the mean flow. The boundary-value problem is thus

$$\nabla^2\psi^{(i)} = 0 \quad \text{for} \quad -\infty < x < \infty, \quad 0 \leqslant y < \infty \tag{5.1}$$

subject to

$$\psi^{(i)}(x, 0; t, y_1) = \pi^{-1} \sin y_1 \sin \pi(x-t), \tag{5.2}$$

$$\psi^{(i)} \to 0 \quad \text{as} \quad y \to \infty, \tag{5.3}$$

where it is understood that this problem has physical significance only for large x although the x domain extends to $-\infty$. To ensure the existence of the x transform, a generalized Fourier transform†

$$\tilde{\psi}^{(i)}(\alpha, y, t, y_1) = \lim_{a\to\infty} \int_{-\infty}^{\infty} \psi^{(i)}(x, y, t, y_1) \exp(i\alpha x - x^2/a^2)\, dx \tag{5.4}$$

is applied to the equation and boundary conditions, where α is the real wavenumber and a is a convergence factor. Solving the ordinary differential equation, applying the boundary conditions and inverting the transform according to

$$\psi^{(i)}(x, y, t, y_1) = \frac{1}{2\pi} \int_{-\infty}^{\infty} \tilde{\psi}^{(i)}(\alpha, y, t, y_1)\, e^{-i\alpha x}\, d\alpha \tag{5.5}$$

yields

$$\psi' = \psi^{(a)} - \psi^{(i)} = \frac{1}{\pi} [\sin(\pi y + y_1) - e^{-\pi y} \sin y_1] \sin \pi(x-t) \tag{5.6}$$

in agreement with (3.22) above. At the wall, $\psi' = 0$ and the impermeability condition is satisfied. As $y \to \infty$, $\psi' \to \psi^{(a)}$ and the original vortex array in the free stream is recovered.

The longitudinal disturbance velocity follows as

$$u' = -\psi'_y = -[\underset{(a)}{\cos(\pi y + y_1)} + \underset{(b)}{e^{-\pi y} \sin y_1}] \sin \pi(x-t). \tag{5.7}$$

At the wall, for the special case $y_1 = -\frac{1}{4}\pi$ the interesting result emerges that $u' = 0$ for all x and t, and thus the velocity field in this inviscid problem also satisfies the no-slip condition as shown in figure 7, where the streamlines of one column for other values of the shifting parameter are also shown. When $y_1 = \frac{1}{4}\pi$, $u' = -2^{\frac{1}{2}} \sin \pi(x-t)$, which is the maximum disturbance speed in the far-downstream domain; the maximum speed in the free stream is unity. Infinite speeds arise at the leading edge, however.

† Although this problem provides experience in the application of this powerful tool, a solution of the form $\phi(y) \sin \pi(x-t)$ can be assumed and $\phi(y)$ then found as the solution of an ordinary differential equation.

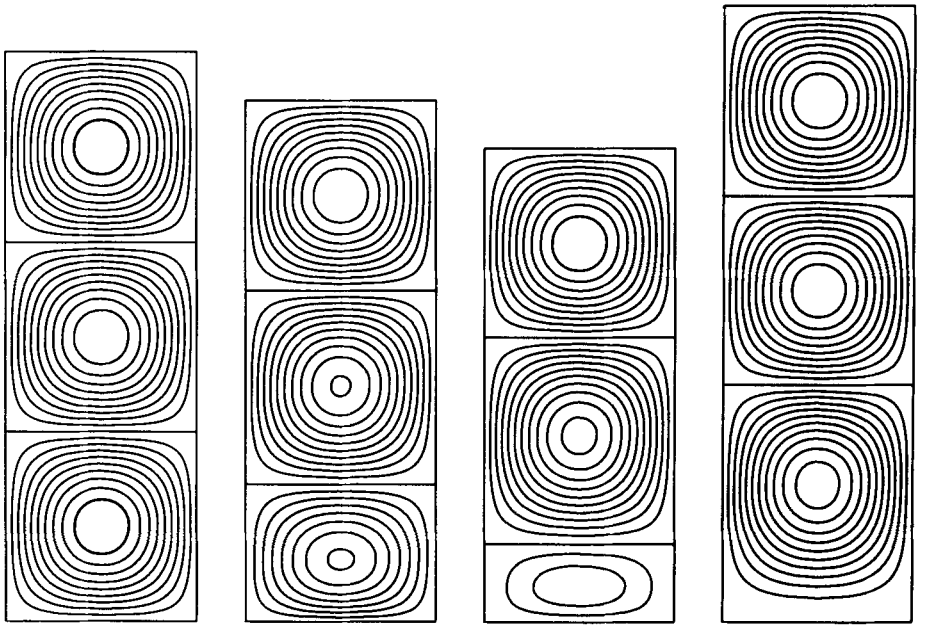

FIGURE 7. Columns of disturbance streamlines for the far-downstream solution for a semi-infinite plate.

6. The counting and boundary paradoxes; the distinction between contours of constant vorticity and streamlines

Several complications arising in the interpretation of eddying flow fields will now be illustrated. The 'counting paradox' is illustrated in figure 8. The question is: are there three or are there four vortices in each column? The left column is the disturbance streamline pattern while the right is the equi-vorticity pattern for the same flow field at the same instant of time and the same position. Whereas the streamlines indicate that there are four vortices, the vorticity pattern indicates that there are three! The structure of the same flow field can be so different when cast in terms of different variables that we identify different numbers of the basic units of structure.

The 'boundary paradox' is shown in figure 9, where the streamlines of 'two' vortices are plotted. If there are two vortices, then the question is: where is the boundary between these vortices? From the left, one dashed line appears to separate the two vortices, while from the right, another seems to be the 'boundary'. The two vortices labelled A and B in figure 9 appear also in figure 5, where it can be seen that vortex B and a third vortex, labelled C, combine to form a fourth vortical system with a single streamline labelled D. Hence the definition of any boundary must allow for several vortical systems to be embedded within one another.

Both paradoxes arise from the confusion associated with the definition of a vortex. The first emphasizes the distinction arising from different variables, while the second illustrates a problem with one variable. The examples illustrate that our intuitive desire to identify 'eddies' or other structures in a turbulent flow requires the investigator

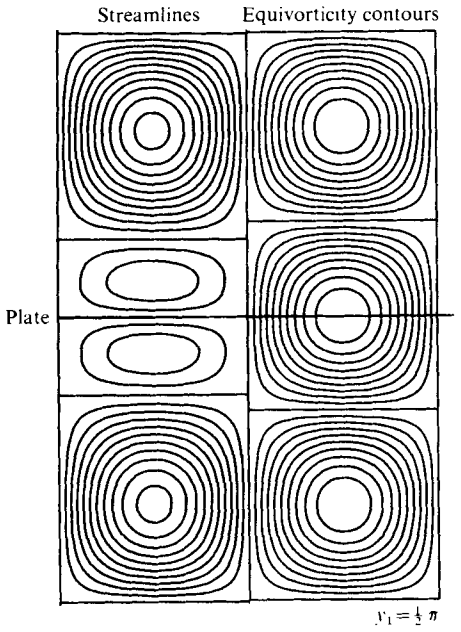

FIGURE 8. The counting paradox. Are there three or are there four vortices?

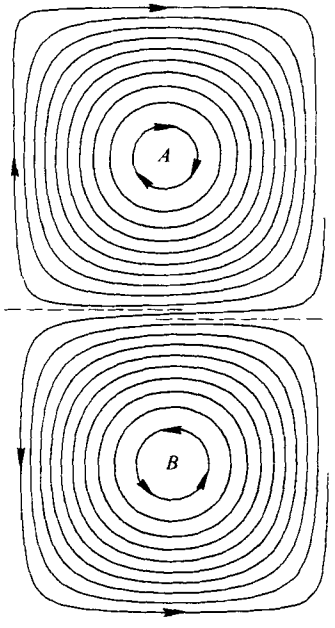

FIGURE 9. The boundary paradox. Where is the boundary between these vortices?

to be sensitive to the variables displayed and to the possibility of vortical systems being embedded within other vortices.

Motivated by these anomalies, we now list several definitions and observations regarding two-dimensional vortices:

(i) A vortex based on contours of constant vorticity (or alternatively, based on

streamlines) occupies the region bounded by the contours of constant vorticity (or contours of constant stream function). It is possible for vortices to be embedded within one another.

(ii) A vortex can be defined on the basis of either closed contours of constant vorticity or streamlines, but the vortices based on the two definitions might not occupy the same space or have common boundaries. The contours of constant vorticity and streamlines coincide if the stream function and vorticity are proportional.

(iii) A vortex based on streamlines is generally different for observers translating at different velocities. If the mean flow is uniform, however, the vortices based on the contours of constant vorticity are the same for all observers in co-ordinate systems which are uniformly translating (but not rotating). The same conclusion also holds for the more general case of irrotational mean flows.

(iv) There is no requirement that either the equi-vorticity contours or the streamlines close (e.g. a plane wave of vorticity in a whole plane). They may close in one direction but remain open in the other direction (thus forming a U-shaped pattern), but these cases will not be considered here.

7. Fluctuating pressure

Like the stream-function and vorticity disturbances, the pressure disturbance can be separated into 'absence' and 'impermeability' contributions: $p' = p^{(a)} - p^{(i)}$. As shown previously (Taylor 1936; V), $p^{(a)} = O(\rho q^2)$ in agreement with many familiar forms of turbulence. In the present analysis, the nonlinear convective terms are $O(q/U_\infty)$ and are neglected relative to the linear terms, which are $O(1)$. Hence to unit order, $p^{(a)} = 0$. This result does not discount pressure variations far away from the plate, which must exist to provide the centripetal force causing a fluid particle to orbit about the vortex centre, but rather means that these pressure variations are associated with the nonlinear terms, which have been neglected.

Consider now the dimensional linearized momentum equations for a uniform mean flow:

$$\frac{\partial u_i'}{\partial t} + U_\infty \frac{\partial u_i'}{\partial x_1} = -\frac{1}{\rho}\frac{\partial p'}{\partial x_i}, \quad i = 1, 2. \tag{7.1}$$

In the vicinity of the leading edge, the velocity field does not generally convect with the mean flow because of the pressure terms. In that region, we *assume* that the sum of the linear inertial terms is not $O(q^2/\Lambda)$ but rather $O(U_\infty q/\Lambda)$ and thus we non-dimensionalize the pressure according to $p' \to \rho q U_\infty p'$. The dimensionless momentum equations are therefore $u_t' + u_x' = -p_x'$ and $v_t' + v_x' = -p_y'$. Now we separate all variables into absence and impermeability components (e.g. $u' = u^{(a)} - u^{(i)}$), obtaining

$$u_t^{(a)} + u_x^{(a)} + p_x^{(a)} = u_t^{(i)} + u_x^{(i)} + p_x^{(i)}, \tag{7.2}$$

$$v_t^{(a)} + v_x^{(a)} + p_y^{(a)} = v_t^{(i)} + v_x^{(i)} + p_y^{(i)}. \tag{7.3}$$

The left-hand sides are zero since the linearized momentum equations also apply far upstream.

Hence $$u_t^{(i)} + u_x^{(i)} = -p_x^{(i)}, \quad v_t^{(i)} + v_x^{(i)} = -p_y^{(i)}. \tag{7.4), (7.5}$$

Following the development of the usual unsteady Bernoulli equation, the potential $\phi^{(i)}$ is introduced, where $u^{(i)} = -\phi_x^{(i)}$ and $v^{(i)} = -\phi_y^{(i)}$, and where $v_x^{(i)} = u_y^{(i)}$ since the

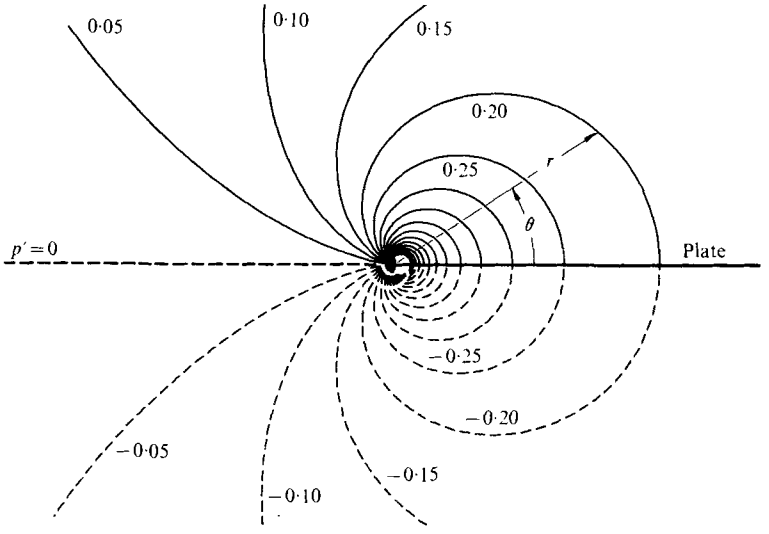

FIGURE 10. Contours of constant pressure arising when an array of vortices impinges on a semi-infinite plate for $y_1 = \frac{1}{2}\pi$ and $t = \frac{1}{4}$. A discontinuity in pressure arises across the plate.

impermeability flow is irrotational. Hence the unsteady linearized Bernoulli equation for the impermeability flow field is

$$-\phi_t^{(i)} + p^{(i)} + u^{(i)} = c(t) = 0. \tag{7.6}$$

Note that the velocity $u^{(i)}$ does not appear squared but rather to the first power. If $\psi^{(i)}$ is known, then the potential $\phi^{(i)} = -i\psi^{(i)}$ can be found, differentiated, introduced into the Bernoulli equation, and the derivatives evaluated, yielding

$$p' = -p^{(i)} = \mathscr{R}\{i \sin y_1 (\cos \pi t + \sin \pi t)/\pi(-2z)^{\frac{1}{2}}\}, \tag{7.7}$$

or alternatively, by letting $re^{i\theta} \equiv z$ where $0 \leqslant \theta < 2\pi$,

$$p' = \cos \tfrac{1}{2}\theta \sin y_1 (\cos \pi t + \sin \pi t)/\pi(2r)^{\frac{1}{2}}. \tag{7.8}$$

Note that this fluctuating pressure vanishes everywhere when $\sin y_1 = 0$, i.e. when the plate coincides with a boundary between the rows of free-stream vortices. It also vanishes along the x axis upstream of the plate and far away from the leading edge in any direction. The pressure oscillates sinusoidally in time with maximum amplitude when $y_1 = \pm \frac{1}{2}\pi$, i.e. when the plate bisects a row of free-stream vortices. Above the plate, the pressure is either a maximum or a minimum when the plate has penetrated through one-quarter of a vortex. Since $p'(z) = -p'(z^*)$, a discontinuity in pressure arises across the plate. A singularity in pressure arises at the leading edge which would be eliminated in practice by local separation, cavitation of a liquid, compressibility of a gas, viscous effects or a finite plate thickness, which would permit a rounded leading edge.

The contours of constant pressure are plotted in figure 10. Note the smooth variation in pressure across the x axis upstream of the plate in contrast to the pressure jump across the plate and the large fluctuations near the leading edge. These contours of constant pressure are similar in shape and can be collapsed into a single curve if the

radial co-ordinate and pressure are further non-dimensionalized with respect to some position x^* along the plate and the surface pressure p^* at that position respectively. Since $p^* = \sin y_1 (\cos \pi t + \sin \pi t)/\pi(2x^*)^{\frac{1}{2}}$, $p'/p^* = \cos(\theta/2)/(r/x^*)^{\frac{1}{2}}$.

In analogy with the double-averages of the velocities, the root double-average of the pressure disturbance can be found as (dimensionally)

$$\overline{\overline{(p'^2)}}^{\frac{1}{2}} = \rho U_\infty q \Lambda^{\frac{1}{2}} |\cos \tfrac{1}{2}\theta| / 2\pi r^{\frac{1}{2}}. \tag{7.9}$$

Note the effect of the vortex scale Λ on the pressure fluctuation.

8. Summary, conclusions and recommendations

The instantaneous flow field associated with an array of vortices convecting downstream towards and alongside a plate has been found. Fundamental changes in the structure of that vortical flow field occur as it encounters the plate. The vorticity fluctuations are distributed, rather than concentrated as point vortices, so as to represent more closely the patches of vorticity, eddies and turbulence encountered in engineering practice. We have focused on the spanwise component of vorticity in this study of unseparated leading-edge effects.

The three domains associated with a vortex array propagating towards and alongside a semi-infinite plate are as follows:

(i) The *free-stream domain*, where the free-stream disturbances are negligibly influenced by the presence of the plate. The iso-vorticity contours and the disturbance streamlines coincide and convect with the mean flow. The vortices line up in straight rows and columns and the disturbance pressure is $O(\rho q^2)$.

(ii) The *leading-edge domain*, which is a transition region between the free-stream disturbances and those far downstream of the leading edge. Significant distortion of the streamline patterns occurs as the plate cuts through the vortices, and relatively large, $O(\rho q U_\infty)$, pressure fluctuations are produced, even though the vorticity pattern is unaffected by the presence of the plate in this linear analysis. The velocities are periodic in time, but not in space. Taylor's hypothesis is generally not valid as a result of the vortices distorting. The vortices intertwine, with some streamlines encircling several vortices. Sometimes, small pieces of a vortex which is cut off-centre by the plate are completely absorbed by a neighbouring vortex. However, the changes in structure depend upon whether one examines the iso-vorticity contours or the disturbance streamlines. While the major adjustment to the plate occurs near the leading edge, the slow algebraic, $O(r^{-\frac{1}{2}})$, decay indicates that the leading edge weakly influences the flow field far away. *Very near* the leading edge and along the plate, viscous and nonlinear effects are significant.

(iii) The *far-downstream domain*, where the vorticity and stream-function fields are periodic in the x direction and in time, but the patterns are different. However, both patterns are composed of straight columns and rows of vortices which are convected along without any further change in structure. The pressure fluctuation is $O(\rho q^2)$. Very near the plate, viscous effects would be important, and nonlinear and viscous effects on the vortices would become increasingly significant further downstream.

The vorticity dynamics are much simpler than the stream function or velocity field in this problem. The vorticity convects with the mean flow, but the stream function is subject to the impermeability condition, which must be applied only along the

$+x$ axis. While the velocity field is quasi-steady and depends only on the instantaneous distribution of vorticity, the pressure field must be found from the unsteady Bernoulli equation and is significantly influenced by the unsteadiness.

Although we have used an array of *square* vortices as our free-stream disturbance, the impermeability stream function (3.15) with the first term removed can be applied to many two-dimensional disturbances with normal velocities which oscillate along the x axis and which satisfy the conditions specified. Such disturbances include oblique plane waves of vorticity, arrays of rectangular vortices and oscillating vortex sheets, but also include *irrotational* fluctuations induced by 'far-away' wavy walls. Effects of phase speeds different from the free-stream velocity, i.e. $c \neq U_\infty$, can be accounted for in the stream function and velocities merely by non-dimensionalizing with c as the characteristic mean velocity, although other effects arise from the pressure. Consequently, what is presented here is a tool for analysing many forms of free-stream disturbance interacting with a plate. Fourier analysis may be used to apply these results with one wavenumber and phase speed to more general periodic or aperiodic disturbances.

Suggestions for future research include studying three-dimensional rectangular prismatic vortices or other three-dimensional disturbances interacting with the leading edges of plates (of zero and finite thickness) and the boundary layer developing along the plate. Detailed numerical and experimental studies of leading-edge effects, including unsteady separation, are also needed.

The author acknowledges stimulating discussions with Dr E. Reshotko, Dr G. Janowitz and Dr R. Arora. A plotting program written by Dr J. Paul was used for figures 3–5, 9 and 10. Financial support was provided by the Air Force Office of Scientific Research under Grants AFOSR-74-2477A & B.

Appendix. Functions in the velocity correlations

The derivatives $\psi'_x = v'$ and $-\psi'_y = u'$ can be found by using the Liebnitz rule to differentiate the Fresnel integrals. The results for the functions associated with the longitudinal velocity in § 4 are

$$\begin{aligned} f_1 &= -\cos\pi x \sin\pi y + \mathscr{I}\{\sin\pi z S_2(-\pi z) - \cos\pi z C_2(-\pi z) \\ &\quad + \sin\pi z C_2(-\pi z) + \cos\pi z S_2(-\pi z) - \sin\pi z + 1/\pi(-2z)^{\frac{1}{2}}\}, \\ f_2 &= \sin\pi z \sin\pi y - \mathscr{I}\{\sin\pi z S_2(-\pi z) - \cos\pi z C_2(-\pi z) \\ &\quad - \sin\pi z C_2(-\pi z) - \cos\pi z S_2(-\pi z) + \cos\pi z - 1/\pi(-2z)^{\frac{1}{2}}\}, \\ f_3 &= \cos\pi x \cos\pi y, \quad f_4 = -\sin\pi x \cos\pi y. \end{aligned}$$

The related functions associated with the normal velocity are

$$\begin{aligned} g_1 &= \sin\pi x \cos\pi y + \mathscr{R}\{\sin\pi z S_2(-\pi z) - \cos\pi z C_2(-\pi z) \\ &\quad + \sin\pi z C_2(-\pi z) + \cos\pi z S_2(-\pi z) - \sin\pi z + 1/\pi(-2z)^{\frac{1}{2}}\}, \\ g_2 &= \cos\pi x \cos\pi y + \mathscr{R}\{-\sin\pi z S_2(-\pi z) + \cos\pi z C_2(-\pi z) \\ &\quad + \sin\pi z C_2(-\pi z) + \cos\pi z S_2(-\pi z) - \cos\pi z + 1/\pi(-2z)^{\frac{1}{2}}\}, \\ g_3 &= \sin\pi x \sin\pi y, \quad g_4 = \cos\pi x \sin\pi y. \end{aligned}$$

REFERENCES

ABRAMOWITZ, M. & STEGUN, I. A. 1965 *Handbook of Mathematical Functions.* Washington: Nat. Bur. Stand.

BATCHELOR, G. K. & PROUDMAN, I. 1954 The effect of rapid distortion of a fluid in turbulent motion. *Quart. J. Mech. Appl. Math.* **7**, 83–103.

CARRIER, G. F. & LIN, C. C. 1948 On the nature of the boundary layer near the leading edge of a flat plate. *Quart. Appl. Math.* **6**, 63–68.

CORRSIN, S. & UBEROI, M. S. 1952 Diffusion of heat from a line source in isotropic turbulence. *N.A.C.A. Tech. Note* no. 2710; *N.A.C.A. Tech. Rep.* no. 1142.

ERDÉLYI, A., MAGNUS, W., OBERHETTINGER, F. & TRICOMI, F. G. 1954 *Tables of Integral Transforms*, vol. 1. McGraw-Hill.

HINZE, J. O. 1959 *Turbulence.* McGraw-Hill.

HUNT, J. C. R. 1973 A theory of turbulent flow round two-dimensional bluff bodies. *J. Fluid Mech.* **61**, 625–706.

LIN, C. C. 1950 On Taylor's hypothesis in wind tunnel turbulence. *Memo. U.S. Naval Ord. Lab.* no. 10775.

LIN, C. C. 1953 On Taylor's hypothesis and the acceleration terms in the Navier–Stokes equations. *Quart. Appl. Math.* **10**, 295–306.

PRANDTL, L. 1933 Attaining a steady air stream in wind tunnels. *N.A.C.A. Tech. Memo.* no. 726 (trans. from Herstellung einwandfreier Luftströme (Windkanäle). *Handbuch Experimentalphys.* **4** (2), 65–106).

ROGLER, H. L. 1974 A mechanism of vorticity segregation. *Bull. Am. Phys. Soc. Ser.* II, **19**, 1165.

ROGLER, H. L. 1975*a* The interaction between vortex-array representations of free-stream turbulence and impermeable bodies. *A.I.A.A. 13th Aerospace Sci. Meeting. A.I.A.A. Paper* no. 75–116.

ROGLER, H. L. 1975*b* The production of higher and lower modes and the decay of an array of vortices near a boundary. *Bull. Am. Phys. Soc. Ser.* II, **20**, 1428.

ROGLER, H. 1977 Free-stream vorticity disturbances adjusting to the presence of a plate – a quarter plane problem. *J. Appl. Mech.* **44**, 529–533.

ROGLER, H. L. & RESHOTKO, E. 1974 Disturbances in a wall boundary layer introduced by an array of low-intensity vortices. *AFOSR Tech. Rep.* no. 74–0795.

ROGLER, H. L. & RESHOTKO, E. 1975 Disturbances in a boundary layer introduced by a low intensity array of vortices. *SIAM J. Appl. Math.* **28**, 431–462. (See also *Proc. Int. Symp. Mod. Develop. Fluid Mech., Haifa, Israel.*)

ROGLER, H. L. & RESHOTKO, E. 1976 Spatially-decaying array of vortices. *Phys. Fluids* **19**, 1843–1850.

TAYLOR, G. I. 1923 On the decay of vortices in a viscous fluid. *Phil. Mag.* **46**, 671–674. (See also *Scientific Papers*, vol. 4, pp. 90–92. Cambridge University Press.)

TAYLOR, G. I. 1935 Turbulence in a contracting stream. *Z. angew. Math. Mech.* **15**, 91–96.

TAYLOR, G. I. 1936 The mean value of the fluctuations in pressure and pressure gradient in a turbulent fluid. *Proc. Camb. Phil. Soc.* **32**, 380–384.

TAYLOR, G. I. 1938 The spectrum of turbulence. *Proc. Roy. Soc.* A **64**, 476–490.

TAYLOR, G. I. & GREEN, A. E. 1937 Mechanism of the production of small eddies from large ones. *Proc. Roy. Soc.* A **158**, 499–521.

VAN DE VOOREN, A. I. & DIJKSTRA, D. 1970 The Navier–Stokes solution for laminar flow past a semi-infinite flat plate. *J. Engng. Math.* **4**, 9–27.

VAN DYKE, M. 1977 Computer extension of perturbation series in fluid mechanics. *Proc. Int. Symp. Mod. Develop. Fluid Mech.*, (*Haifa, Israel* (1973), (ed. J. Rom), pp. 174–188.